

Recent Progress and Future Advances on Aqueous Monovalent-Ion Batteries towards Safe and High-Power Energy Storage

Fangli Zhang, Wenchao Zhang,* David Wexler, and Zaiping Guo*

Aqueous monovalent-ion batteries have been rapidly developed recently as promising energy storage devices in large-scale energy storage systems owing to their fast charging capability and high power densities. In recent years, Prussian blue analogues, polyanion-type compounds, and layered oxides have been widely developed as cathodes for aqueous monovalent-ion batteries because of their low cost and high theoretical capacity. Furthermore, many design strategies have been proposed to expand their electrochemical stability window by reducing the amount of free water molecules and introducing an electrolyte additive. This review highlights the advantages and drawbacks of cathode and anode materials, and summarizes the correlations between the various strategies and the electrochemical performance in terms of structural engineering, morphology control, elemental compositions, and interfacial design. Finally, this review can offer rational principles and potential future directions in the design of aqueous monovalent-ion batteries.

nature and instability. Among the various energy storage technologies and devices, rechargeable batteries have been extensively developed as the most promising and reliable devices for a diverse range of applications, from microchips to vehicles and stationary energy storage devices. The commercial lithium-ion batteries (LIBs) with high energy density, long lifespan, and fast charge–discharge capability have been widely used in portable electronic devices, (hybrid) electric vehicles, and even in grid-scale energy storage facilities.^[2] Nevertheless, future applications of LIBs are still hindered by the scarcity of Li, safety risks, and environmental challenges due to the use of volatile, flammable, and toxic organic electrolytes.


The use of aqueous-based electrolytes in batteries has been attractive for large-

scale energy storage owing to their intrinsic safety, environmental benignity, easy fabrication, and low cost,^[3] but their potential applications have been impeded by two major issues, their limited energy density and their unsatisfactory life span. Unlike the nonaqueous electrolytes, the narrow stable electrochemical window (ESW) of 1.23 V in aqueous electrolytes is due to their inherent thermodynamic oxidation potential (oxygen evolution reaction [OER]) and reduction potential (hydrogen evolution reaction [HER]), as well as water-based side reactions between oxygen/hydrogen and the electrodes,

1. Introduction

With the rapid depletion of fossil fuels and the environmental pollution caused by their burning, the development of alternative renewable energy sources such as wind, solar, and tidal energy is becoming an inevitable trend and in the spotlight to meet increasing energy demands.^[1] Therefore, low-cost and high-performance energy storage devices are urgently needed to effectively power vehicles and achieve large-scale energy storage of this renewable energy because of its intermittent

F. Zhang
Institute for Superconducting & Electronic Materials
Australian Institute for Innovative Materials
University of Wollongong
Innovation Campus
North Wollongong, New South Wales 2500, Australia

 The ORCID identification number(s) for the author(s) of this article can be found under <https://doi.org/10.1002/adma.202107965>.

© 2022 The Authors. Advanced Materials published by Wiley-VCH GmbH. This is an open access article under the terms of the Creative Commons Attribution-NonCommercial-NoDerivs License, which permits use and distribution in any medium, provided the original work is properly cited, the use is non-commercial and no modifications or adaptations are made.

DOI: 10.1002/adma.202107965

W. Zhang
School of Metallurgy and Environment
Central South University
Changsha 410083, China
E-mail: wenchao.zhang@csu.edu.cn

W. Zhang
Chinese National Engineering Research Centre for Control & Treatment of Heavy Metal Pollution
Changsha 410083, China

D. Wexler
Faculty of Engineering and Information Science
University of Wollongong
Northfields Ave
Wollongong, New South Wales 2522, Australia

Z. Guo
School of Chemical Engineering & Advanced Materials
The University of Adelaide
Adelaide, South Australia 5005, Australia
E-mail: zaiping.guo@adelaide.edu.au

which seriously limit the choice of electrode materials.^[4] To date, Prussian blue and its analogues, polyanion-type compounds, and oxides have been extensively studied as cathodes for aqueous-based batteries due to their ease of synthesis, open framework structure, chemical stability, tuneable redox potentials, and excellent electrochemical activity, although these cathode materials generally suffer from poor cycling stability and low energy density. In the case of the anode materials, conventional inorganic anode materials, such as polyanionic compounds and oxides, have been greatly impeded by their inherent poor electronic conductivity or structural cycling instability. In contrast, organic anodes are considered as the most promising candidates because of their structural diversity, robust stability, design flexibility, and low cost, but the research on organic anodes in aqueous batteries is currently in its infancy, and there are few studies related to the fundamental relationship between the structure of organic anodes and the corresponding electrochemical performances.

Compared with nonaqueous batteries, the outstanding ionic conductivity (twice as high as for organic electrolytes) of aqueous electrolytes could allow fast charging capability and high power densities.^[5] More importantly, the hydrated ionic radius and hydration free energy are the key factors that determine the chemical diffusivity in liquids and solids. On the one hand, ionic diffusion in aqueous solution is in the form of individual hydrated ions with first hydration shells, and the hydrated ionic radius has a strong correlation with ionic diffusivity. As shown in **Figure 1a**, monovalent ions exhibit faster ion diffusion rates in aqueous electrolytes due to their smaller hydrated ionic radius than those of multivalent ions.^[6] On the other hand, hydrated ions require energy to remove the water molecules surrounding them at electrode/electrolyte interfaces

and then to insert themselves into the structure. The hydration free energy is a measure of the stability of the hydrated ions in relation to the weak bonding between the ions and the water molecules forming the hydration shell. Monovalent ions with lower hydration free energy can shed water molecules more easily than multivalent ions. Therefore, monovalent-ions as charge carriers in batteries exhibit fast diffusion kinetics both in aqueous electrolytes and at electrode/electrolyte interfaces compared with multivalent metal ions.^[7] Therefore, aqueous monovalent-ion batteries may offer great benefits for high power devices.

The past few years have witnessed notable progress on aqueous-based batteries from the aspects of fundamental reaction mechanisms and enhanced electrochemical performance in various electrode/electrolyte systems. Many review papers have summarized the recent progress and achievements on electrode and electrolyte materials,^[8] but few review papers have outlined strategies to address our fundamental understanding of the disadvantages of different electrode materials and their narrow voltage windows. Moreover, the correlations between the strategies and the performance are still unclear, which makes it difficult to help researchers by providing design principles for electrodes and electrolytes. In this review, we summarize recent progress and achievements on aqueous monovalent-ion batteries, and the fundamental reaction mechanisms of various electrode materials in aqueous electrolytes are also discussed from the perspectives of molecular structure, morphology, elemental compositions, and the electrode/electrolyte interphase. On the basis of the strategies encountered in different systems, solutions to the current bottlenecks, promising design principles, and future research directions in aqueous monovalent-ion batteries will be proposed.

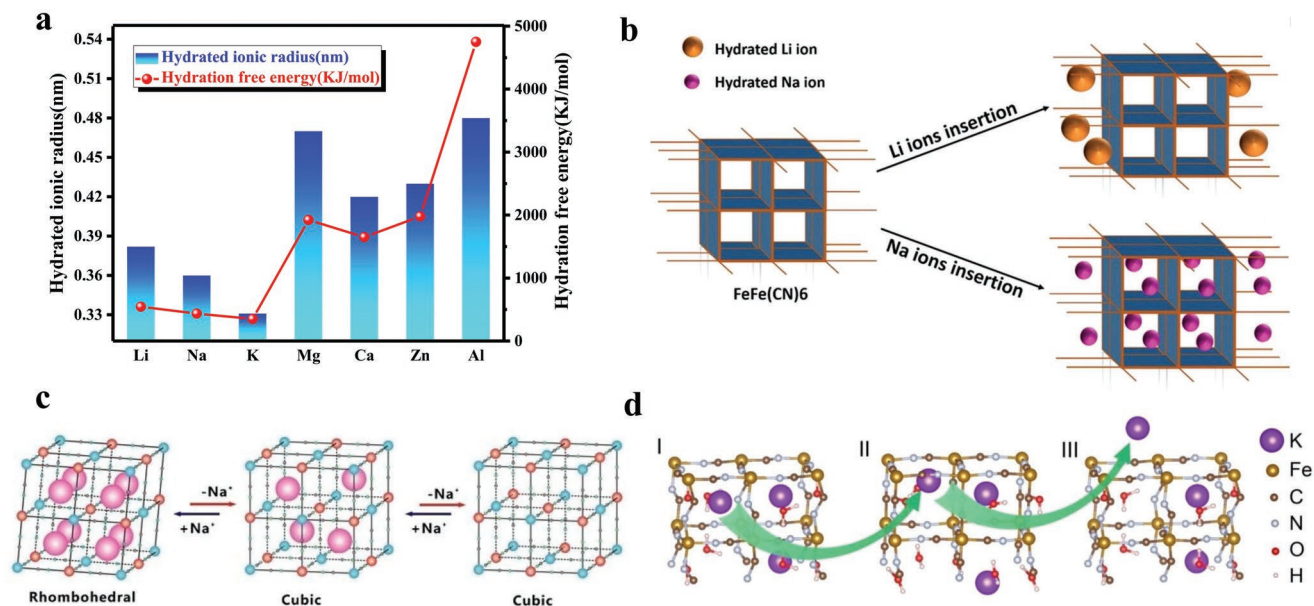


Figure 1. a) A comparison of ionic radius and hydrated ionic radius of univalent and multivalent metal ions. b) Schematic illustration of Na ion and Li ion insertion into FeFe(CN)₆. Reproduced with permission.^[12b] Copyright 2018, Elsevier Ltd. Structural evolution of c) rhombohedral Na₂Co^{II}Fe^{II}(CN)₆. Reproduced with permission.^[15a] Copyright 2015, Wiley-VCH; and d) orthorhombic K₂Fe^{II}[Fe^{II}(CN)₆]₂·2H₂O. Reproduced with permission.^[12a] Copyright 2016, Wiley-VCH.

2. Cathode Materials in Aqueous Monovalent-Ion Batteries

2.1. Prussian Blue (PB) and Its Analogues

Prussian blue (PB) and its analogues (PBAs) have been widely investigated due to their high theoretical energy density and outstanding rate performance.^[9] The chemical composition of PBAs can be expressed as $A_xP_y[R(CN)_6]_{1-z}z\Box \cdot mH_2O$ (A = alkali metal; P , R = transition metal; \Box = vacancy).^[10] Large interstitial sites within the open framework can host monovalent-ions and/or zeolitic water, while the 3D channels provide a fast diffusion pathway for ion transportation.^[11]

In PBAs, the insertion/extraction mechanisms of the hydrated monovalent ions are controlled by two processes, the Faradaic intercalation process and the capacitive response.^[12] The Faradaic intercalation process dominates for hydrated K and Na ions, while the capacitive-controlled process dominates for hydrated Li ions, owing to their different hydrated ion size. Larger hydrated Li ions are more likely to occupy the large open sites on the electrode surface, while smaller hydrated Na and K ions tend to occupy the interstitial sites in the lattices of PBAs (simulated in Figure 1b).^[12b,c] Meanwhile, the charge transfer resistance (R_{ct}) of PBAs is the lowest in aqueous potassium electrolytes compared with those in lithium and sodium electrolytes, indicating fast kinetics and low polarization. Hence, PBAs in aqueous potassium batteries might exhibit excellent electrochemical behavior.

The practical applications of PBAs have been restricted, however, by poor utilization of their electrochemical capacities and unsatisfactory reversibility. The defects and $[Fe(CN)_6]$ vacancies that are coordinated by zeolitic water in the PBA crystal structure could block off the active sites for the storage of monovalent ions, which results in low utilization of their electrochemical capacities. Rapid nucleation and lattice growth in the coprecipitation process could lead to the formation of defects and vacancies. To suppress the growth rate, optimizing experimental parameters and developing novel synthesis methods such as etching methods have been proposed.^[13] For example, adding citrate ions during the coprecipitation process could decelerate crystallization and the corresponding separation of the nucleation and growth stages.^[14] Similarly, vacancy-free $Na_2CoFe(CN)_6$ nanocubes and low-defect $FeFe(CN)_6$ nanocrystals have been synthesized by a controlled crystallization reaction and a slow chemical precipitation method, respectively.^[15]

Collapse of the framework structure, complicated phase transitions, and dissolution of transition metals during cycling are the major reasons for poor reversibility. Monovalent-ion rich PBAs deliver high energy density because they are capable of storing up to two monovalent ions per formula unit and undergo two one-electron redox processes corresponding to successive redox reactions of $R^{III/II} - C$ and $P^{III/II} - N$ couples (when R , P = Mn, Fe, Co, etc.) compared to PBAs with a higher oxidation state of the transition metal P (e.g., $Na_2NiFe(CN)_6$ and $Na_2CuFe(CN)_6$).^[15,16] From the viewpoint of elemental composition design, researchers have found that a high amount of monovalent ions could increase the redox capacity but also lead to an irreversible and complicated phase transition during

cycling. PBAs usually possess a face-centered cubic phase, but distortions to monoclinic and rhombohedral structures have been observed in PBA crystals after accommodating too many monovalent ions. For example, with increasing monovalent-ion content, the lattice of Na-rich PBAs changes from cubic to monoclinic and then to rhombohedral. Furthermore, it experiences a phase transition from the rhombohedral structure to face-centered-cubic during cycling (Figure 1c),^[15a,17] while the lattice of K-rich PBAs is distorted to monoclinic or orthorhombic symmetry but can maintain highly reversible phase changes during cycling (Figure 1d).^[12a,18] The complicated mechanisms of these phase transitions in aqueous batteries have remained unclear.

From the perspective of crystal structure design, it was found that water in the PBA lattice, residing at the center of the void spaces in the PBA lattice (Figure 2a), may serve as pillars to maintain the crystal structure during electrochemical cycling and facilitate low strain in charge/discharge processes for aqueous Na ion batteries.^[19] Hydrated PBAs are predicted from first-principles calculations to exhibit a more stable phase transition behavior (Figure 2b) than their dry counterparts over a wider range of Na chemical potentials and small volume changes during cycling (Figure 2c).^[20] Therefore, the desired target for high-performance PBAs is that they should possess low vacancies and low amounts of water residing in the void spaces of the lattice.

In addition, the substitution of inactive/electroactive elements has been applied to stabilize the structure of PBAs, such as by doping with 23% Ni^{2+} in Na-rich PBAs and Fe-substituted Mn in K-rich PBAs,^[20a,21] so further investigations should focus on explaining the charge-transfer mechanisms after the substitution of different elements, and this should be extended to investigations using other elements. On the other hand, the PBA framework structure could be protected from structural collapse and metal ion dissolution by introducing electrolyte additives, for example, $Na_2CoFe(CN)_6$ in an electrolyte modified by adding 1 wt% $CoSO_4$ in 1 M Na_2SO_4 . The batteries with modified electrolyte exhibited superior cycling stability compared with those with blank electrolyte.^[22]

2.2. Polyanion-Type Compounds

Polyanion-type electrode materials can be defined as a class of compounds that contain a series of tetrahedral anion units $(XO_4)^n$ or their derivatives $(X_mO_{3m+1})^n$ (X = S, P, Si, As, Mo, or W) with strong covalent-bonded MO_x polyhedra (where M represents a transition metal).^[23] Their special open framework offers large ion channels for monovalent-ion diffusion,^[24] and the strong X–O covalent bonds significantly improve the stability of O in the lattice, leading to high theoretical energy capacity and long cycling performance. The practical application of polyanion-type compounds has been limited, however, by their poor rate performance due to their intrinsic low electronic conductivity.

Numerous attempts have been proposed to increase the rate performance of PBAs via elemental composition, morphology, and electrode/electrolyte interphase design. From the perspective of composition design, research has focused on developing

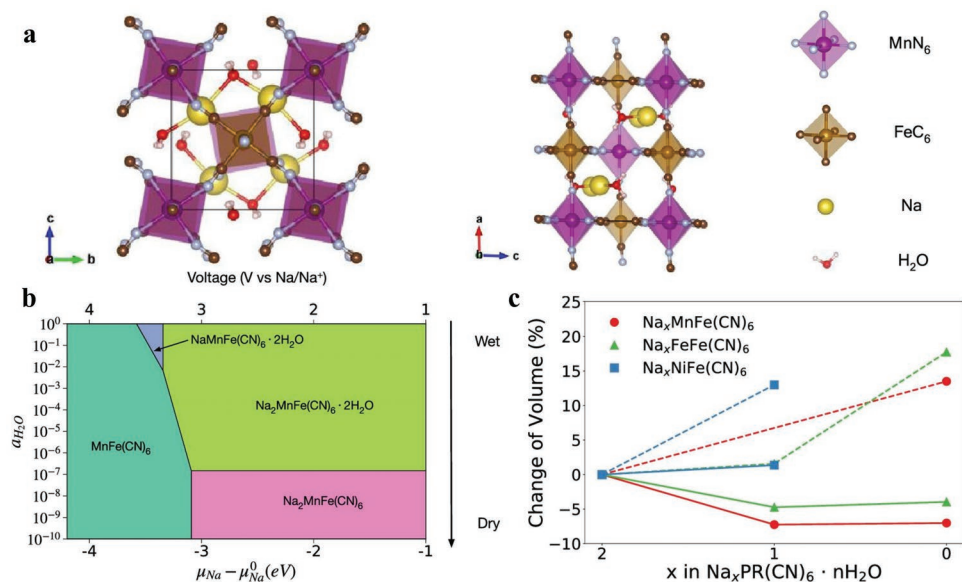


Figure 2. a) Optimized structure of $\text{Na}_2\text{MnFe}(\text{CN})_6 \cdot 2\text{H}_2\text{O}$. b) Grand potential phase diagram of $\text{Na}_x\text{MnFe}(\text{CN})_6 \cdot n\text{H}_2\text{O}$. c) Volume changes of PBAs from Na deintercalation in wet (solid line) and dry (dashed line) electrolytes. Reproduced with permission.^[20] Copyright 2019, American Chemical Society.

nanosized composites with high-electronic-conductivity materials to optimize their rate capacity. Composites with carbon have been extensively studied, from the simple formation of composites with carbon to further tailoring the carbon structure and morphology, as in the case of multi-walled carbon nanotubes (MWCNTs), single-walled carbon nanotubes (SWCNTs), etc.^[25] Graphene, graphene oxide, and reduced graphene oxide have also been found to be good choices to form composites.^[26] Future optimization could involve discovering new inexpensive materials for substitution, tailoring the carbon morphology to form a uniform matrix, modifying carbon, such as by heteroatom doping or nitrogen-doping, and the selection of varied nitrogen sources.^[27] In addition, tailoring polyanion-type compounds into highly conductive substrates and constructing the architecture of the substrate so as to shorten electron transport paths could be proposed to enhance the low electronic conductivity.

Enhancing ionic conductivity is an effective approach to improving rate performance. In terms of the morphology design, shortening the ion diffusion distance and increasing the surface area between the electrode and the electrolyte could facilitate ion diffusion. Synthesis methods and experimental parameters are decisive for sample morphology. Solid-state reaction just involves a simple process to obtain products with high crystallinity, but the products always suffer from topographical irregularity and being of a large size, which strongly restricts the efficient transfer of electrons and increases the interface resistance. The sol-gel method was then developed to reduce the particle size,^[28] although the subsequent high-temperature annealing process still inevitably resulted in increased particle size and the formation of irregular morphology. Therefore, the development of novel synthesis methods, and improvements and/or combinations of conventional methods to fabricate products that are nanosized, highly crystalline, and have ideal morphology could be the current trend and focus.

From adding synthetic agents such as poly(vinyl alcohol) and oxalic acid to combining two synthesis methods, such as in the hydrothermal assisted sol-gel approach,^[29] the target has been smaller particle size and high surface area, which can help to enhance the electrode/electrolyte contact and promote ion-diffusion during cycling. More detailed tailoring and engineering could be applied in the morphology design, including ideal porous surface phases and special preferred orientations of the crystal structure. Well-aligned cross-linked $\text{Na}_2\text{VTi}(\text{PO}_4)_3$ /porous carbon nanofiber is an excellent example.^[30] A modified electrospinning system with an electrospinning emitter and a metal-mesh receiver has been set up to fabricate the aligned cross-linked 1D nanoarchitecture. On the one hand, the single nanofibers demonstrated a highly porous and hierarchical architecture, which not only facilitates highly efficient electrolyte penetration, but also enables fast ion transport. On the other hand, the nanofibers were arranged in a good alignment along two crossing directions and interconnected to form a 3D network with rhombic voids on a large centimeter scale. Compared with the disordered electron transport in randomly arranged nanofibers, the highly oriented pathways could enable fast electron transport capability for the crosslinked architecture, resulting in its high conductivity. These structural and morphological advantages led to high structural stability, thus better cycling durability and superior high-rate properties, which proves the importance of structure and morphology design based on the development of novel synthesis methods.

Interphase modification is another way to improve rate performance by coating materials with high electronic conductivity such as carbon and AlF_3 on the cathode surface and using an additive to modify surface properties, as in the case of CeO_2 -modified LiFePO_4 .^[29a,b,31] Meanwhile, highly concentrated electrolytes with selected anions, such as CF_3SO_3^- , not only can increase the ionic conductivity but also provide more carrier ions for insertion/extraction, corresponding to better

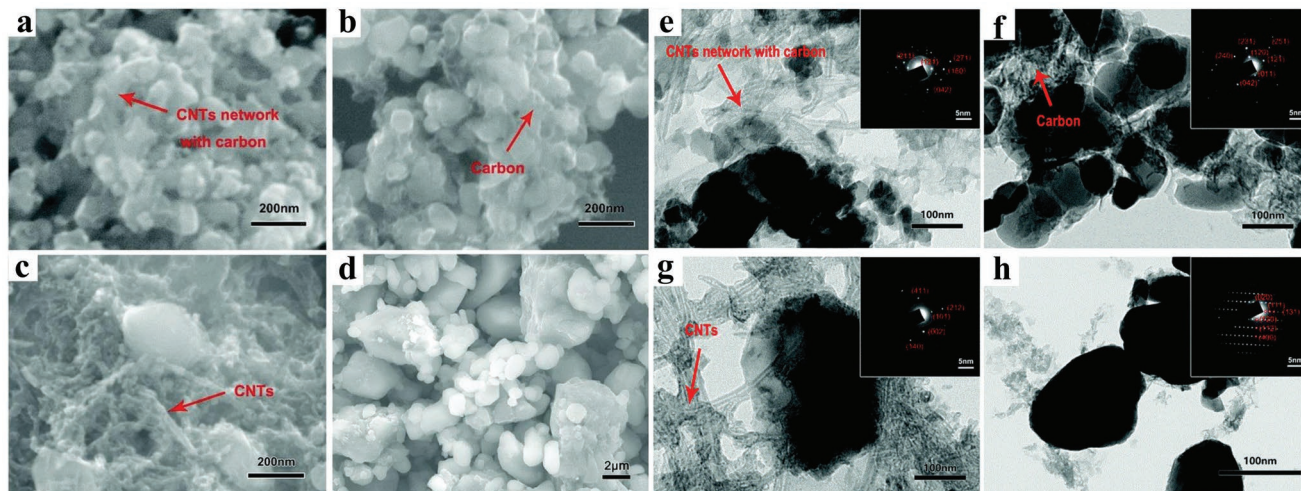


Figure 3. Scanning electron microscope (SEM) images: a) LiFePO₄/C/CNTs, b) LiFePO₄/C, c) LiFePO₄/CNTs, and d) LiFePO₄. Transmission electron microscope (TEM) images of composites: e) LiFePO₄/C/CNTs, f) LiFePO₄/C, g) LiFePO₄/CNTs, and h) LiFePO₄, with the inset images showing the corresponding selected area electron diffraction (SAED) patterns. Reproduced with permission.^[34] Copyright 2020, the Owner Societies.

energy density.^[32] Recently, combinations of several strategies have been popular and widespread to enhance the overall electrochemical performance.^[33] One example is LiFePO₄/C/CNT material combined with composite and coating strategies.^[34] With the addition of carbon nanotubes (CNTs), the nano/micro-sized particles are covered with a flocculent carbon layer connected to a 3D network (as shown in **Figure 3a–d**), which can not only shorten the diffusion distance for Li-ions from the cathode bulk phase to the electrolyte, but also buffer volume expansion during charging and discharging. The amorphous character of LiFePO₄/C/CNTs (**Figure 3e–h**) can reduce the contact resistance between the electrode and the electrolyte. All the above features lead to outstanding rate performance and cycling stability.

2.3. Layered Oxides

Oxides have been considered as among the most promising candidates for cathodes in aqueous monovalent-ion batteries, which include spinel oxides, perovskite oxides, and layered oxides. Among them, layered oxides have attracted much attention due to their high rate performance with 2D pathways and excellent theoretical capacity. Their formula can be expressed as A_xMO₂ (0 ≤ x ≤ 1), where M stands for transition metal elements. The crystal structures are built up from MO₂ sheets of edge-sharing MO₆ octahedra, where the monovalent ions are inserted into and out of the layers between the MO₂ sheets.

The main drawback of layered oxides is their structural instability during cycling, which is caused by complicated phase transitions, collapse of stacked layers, the dissolution of transition metal ions into aqueous electrolytes, and side reactions taking place at the electrode/electrolyte interphase. The nature and content of A cations is one of the decisive factors that determine the crystal structure and phase transitions of layered oxides. In layered lithium oxides, the most prevalent phase transition is from the O3 to the O1 phase after complete Li removal. Transformations to one or more hybrid

O1/O3 phases may also occur at intermediate compositions (as shown in **Figure 4a**).^[35] In layered sodium oxides, the crystal structure type is largely determined by the Na content: P2 layered structures for 0.33 < x < 0.9, and O3 layered structures for 0.9 < x < 1 (**Figure 4b**).^[36,37] With the extraction of Na ions, the O3 phase often undergoes more complex phase transitions than the P2 structure, such as O3→O'3→P3→P'3→P3'' for NaNi_{0.5}Mn_{0.5}O₂, while the P2 phase commonly shows one P2–O2 phase transition.^[37] In layered potassium oxides, the structure type strongly depends on the K/M ratio: O3 phase for K/M = 1, and P2 or P3 phases for K/M ≤ 1 (**Figure 4c**).^[38] There are few studies, however, on detailed phase transitions of layered oxides in aqueous solution.

The complicated reasons for induced capacity fading include spontaneous oxidation, where oxidation of the aqueous electrolyte by the charged layered oxide cathode results in irreversible capacity loss,^[39] and metal ion dissolution, when monovalent ions are exchanged with H⁺ on exposure to water, which are critical problems that need to be investigated urgently. Past research found that layered oxides, including most O3 and P2 layered oxides,^[39,40] possess high reactivity with the atmosphere, such as with air or water, but it should be noted that P2 oxides with superstructure ordering of the transition metals are air- and water-stable. Therefore, future research should be focused on the relationship between the crystal structure and the chemical stability of layered oxides and on developing ideal material systems. Layered oxides generally suffer from unfavorable transition-metal slab sliding due to their strong transition-metal layer interaction in the highly de-sodiated state, which could cause large internal stress and subsequent collapse of the structure. The “pinning effect” from alloy science could be introduced to enhance the structural stability of layered oxides.^[41] Doping an appropriate proportion of metal atoms, such as Fe, Co, and Ni,^[42] to occupy the monovalent-ion layer could be used to create pinning points to inhibit the adverse slab-slipping during cycling.

Based on studies of their crystal structure, researchers found that hydrated layered oxides should be attractive choices

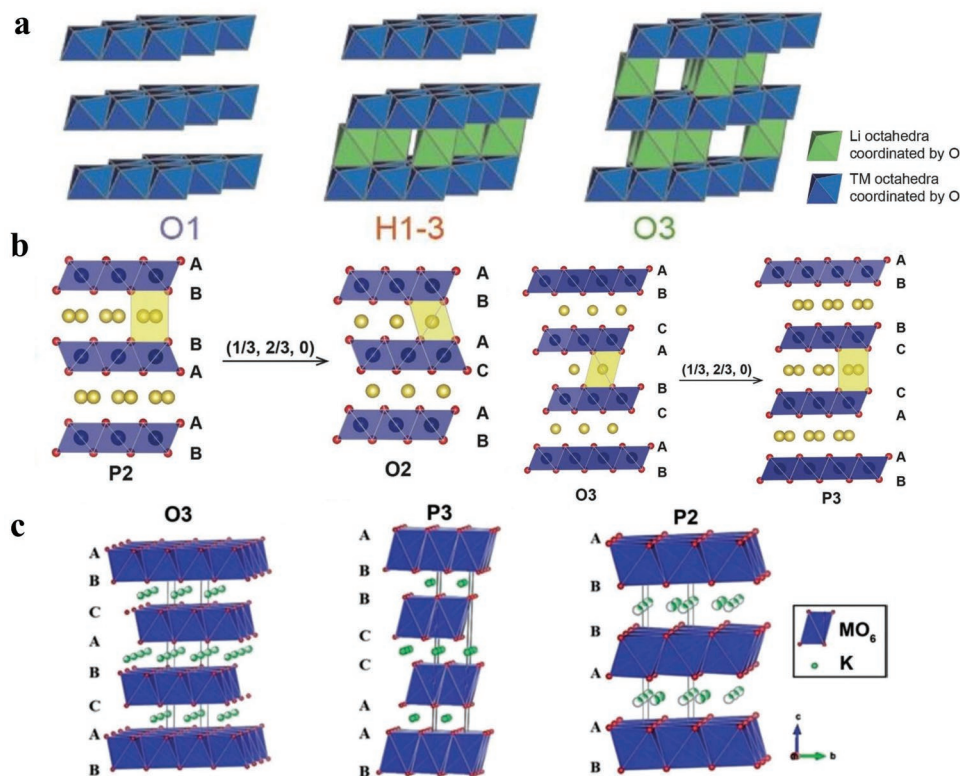


Figure 4. Schematic illustration of the crystal structures of a) layered lithium oxides. Reproduced with permission.^[35] Copyright 2017, WILEY-VCH; b) layered sodium oxides. Reproduced with permission.^[37b] Copyright 2017, WILEY-VCH; and c) layered potassium oxides. Reproduced with permission.^[38b] Copyright 2020, WILEY-VCH.

because structural water within the interlayer can increase the interlayer spacing to facilitate fast ion diffusion and stabilize the structure as pillars during cycling, leading to better rate performance and long cycling lifespans.^[43] They can be synthesized by an aqueous sol-gel route or after initial cycling in aqueous electrolytes. Furthermore, their high degree of hydration can improve the electrochemical activity by increasing the reordering of the local structure and the coherence length.^[44] As shown in **Figure 5a**, fully hydrated materials demonstrate a greater increase in intensity of their O-H bonds ($r = 1 \text{ \AA}$), and there are new O-O features at a radial distance of 4–6 Å. Apart from structural water, it has been found that the capacity fading of layered oxides is related to the local structural distortion during cycling. Through studying the crystal structure of LiCoO₂ on the atomic scale, it has been observed that the presence of protons that occupy the Li ion sites in the layered LiCoO₂ led to distorted CoO₆ octahedra (Figure 5b), which will cause large electrode polarization and fast capacity fading.^[45]

Hierarchical architecture and hollow morphology can not only retain the metrics of the stacked multilayer nanosheets, leading to structural stability, but also further shorten the ion diffusion distance and enhance the specific capacity by their low density. As is well known, the synthesis method and experimental parameters are critical factors for material morphology. K_{0.27}MnO₂ with a flower-like architecture was synthesized by a facile topochemical method, and hollow K_{0.27}MnO₂ nanospheres (Figure 5c,d) were fabricated by a modified polymerization reaction using nanospherical polystyrene (PS) as the

template. Their performance proved the importance of hierarchical architecture and hollow morphology.^[46] These preceding findings have offered us good directions for future study, but there are still several experimental parameters that need to be understood to realize the full potential of layered oxides, such as the calcination temperature, selection of solvents and their concentration, etc. Therefore, it is essential to understand the effects of experimental parameters on the morphology via advanced characterization tools and to develop novel synthesis methods to optimize the morphology of layered oxides.

From the perspective of elemental composition design, both transition-metal ion substitution and the use of additional components are popular strategies to improve the electrochemical properties of layered oxides.^[47] Doping with relatively stable elements, such as Fe, Ni, Ti, etc., is a common way to increase the cycling stability of layered oxides. Future optimization of elemental composition design could involve the joint substitution of several elements, optimizing the amounts of substituted elements, and obtaining a deep understanding of the detailed mechanisms of different elements in relation to the crystal structure and phase transitions. For instance, Kumar et al. studied the effects of partial or complete substitution of Ti for Mn to prove that Ti-doping can significantly improve the stability of O3-type Na-T_M-oxides against hydration and cyclic stability by suppressing the higher impedance and voltage hysteresis that appear with battery cycling.^[47c] In the case of Na_{0.44}MnO₂-CNT composites, it has been proved that the thin layer of CNTs wrapped around the surfaces of Na_{0.44}MnO₂ significantly improve the

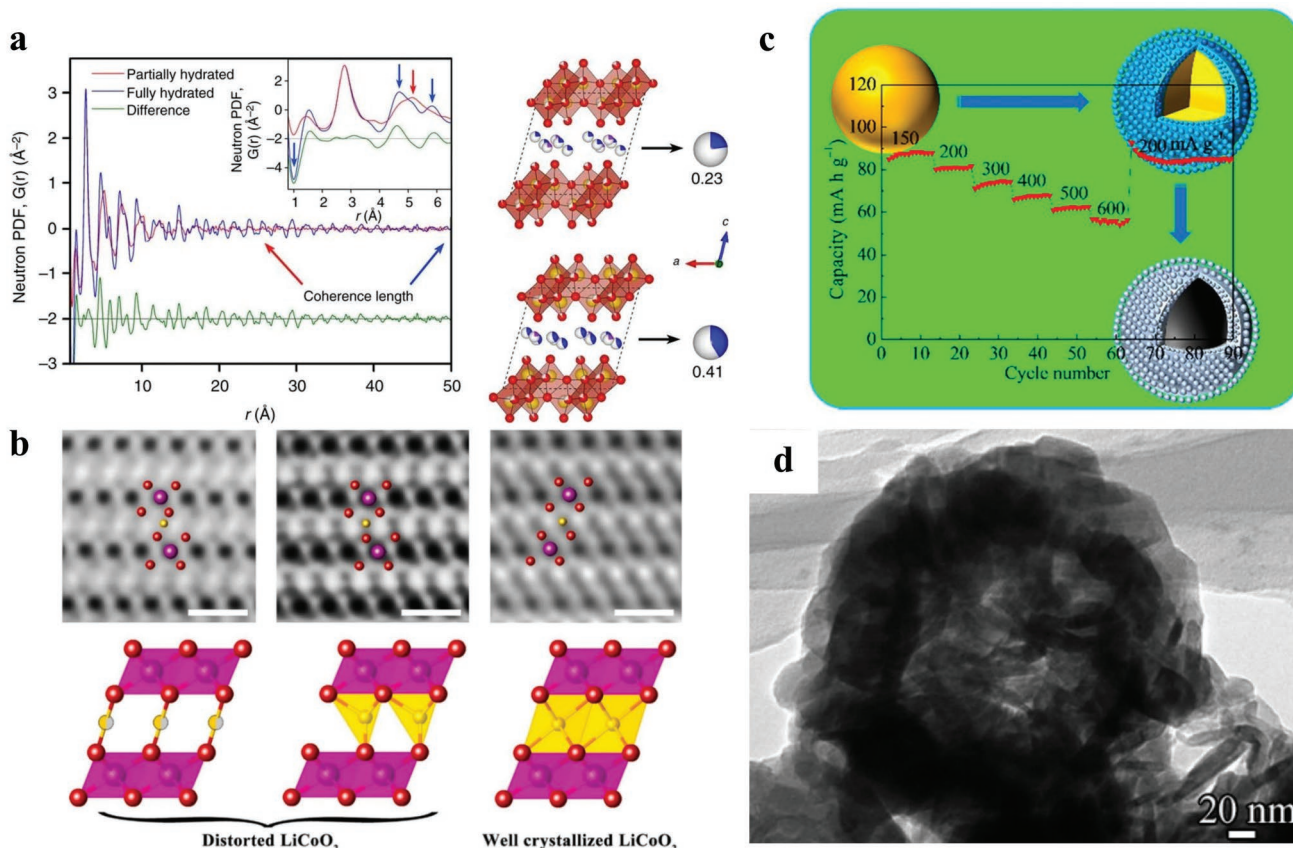


Figure 5. a) Experimentally collected neutron pair distribution function (PDF) curves of partially and fully hydrated disordered potassium vanadium oxide (KVO) and the refined local structure of partially and fully hydrated KVO materials. Schematic illustration of the synthesis procedure for LiCoO_2 nanosheets assembled with nanorod arrays on carbon cloth. Reproduced with permission.^[44] Copyright 2017, the author(s). b) Annular bright field (ABF) images and lattice structure of CoOOH (left), distorted LiCoO_2 (middle), and well-crystallized LiCoO_2 (right). Reproduced with permission.^[45a] Copyright 2018, Elsevier Ltd. c) Schematic illustration of the fabrication of hollow $\text{K}_{0.27}\text{MnO}_2$ nanospheres. d) TEM image of $\text{K}_{0.27}\text{MnO}_2$. Reproduced with permission.^[46b] Copyright 2016, American Chemical Society.

electronic conductivity and the cathode stability during charging and discharging processes, because CNTs can help $\text{Na}_{0.44}\text{MnO}_2$ particles to keep close contact with each other.^[47d]

3. Anode Materials in Aqueous Monovalent-Ion Batteries

Because suitable anode materials with satisfactory capacity and proper operating potential in aqueous electrolytes are limited, there is an urgent need to find candidate materials to build aqueous monovalent-ion batteries for practical applications. Polyanionic compounds show low voltage plateaus and stable 3D framework structures in aqueous solution, but their intrinsic poor electronic conductivity restricts their rate performance.^[48] Carbon coating, composites, and substitution are effective methods to overcome this issue. From simply carbon coating to further optimizing the composition and structure of carbon, numerous attempts have been proposed to further enhance their electronic conductivity.^[49] Zhao et al. coated crystals with hierarchical carbon, which consisted of a nanoscale carbon layer and a microscale carbon network, to increase the surface area and pore volume (Figure 6a).^[50] Researchers found

that a nitrogen-doped carbon coating could improve the electronic conductivity and generate defects for insertion/extraction of monovalent ions.^[51] Based on this discovery, they studied the influence on the electrochemical performance of different synthesis methods in depth and varied their carbon and nitrogen sources, such as urea, tripolycyanamide, ethylenediamine, polyaniline, and polydopamine.^[52] In order to accelerate electron and ion transport between particles, the desired composites should consist of particles dispersed in a graphene matrix or carbon matrix.^[53] Jiang et al. synthesized a graphene-decorated $\text{NaTi}_2(\text{PO}_4)_3/\text{C}$ composite to achieve better rate capacity, which benefited from the high conductivity of carbon and the larger surface area of graphene.^[54] Small grain size, uniform dispersion, less agglomeration, and porous structure constitute an ideal morphology to enhance electron and ion diffusion. Through different synthesis methods, more detailed tailoring of the morphology can be obtained. For example, $\text{NaTi}_2(\text{PO}_4)_3/\text{C}$ composite was prepared by a self-assembled synthesis, which possessed an outer plate-like morphology and an internal 3D porous-structured conductive matrix, forming bicontinuous pathways for fast electron transport.^[50]

Oxides as anode possess unique layered structures, which can provide fast diffusion channels for monovalent ions to

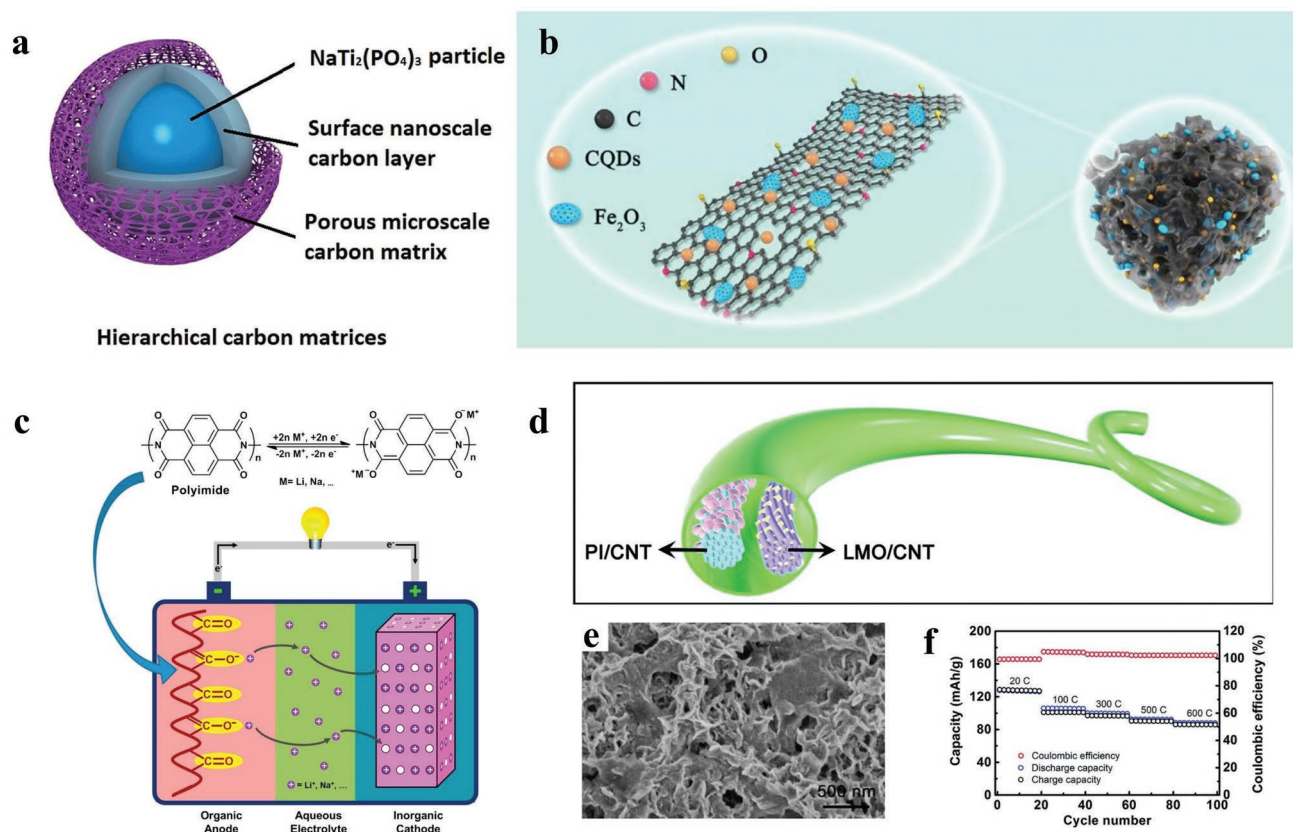


Figure 6. a) Schematic image of bicontinuous pathways in a hierarchical carbon matrix for highly-efficient electron/ion transport in a wafer-like architecture. Reproduced with permission.^[50] Copyright 2015, The Royal Society of Chemistry. b) Schematic illustration of the structure of N-CQDs/rGO/Fe₂O₃ composite aerogel. Reproduced with permission.^[56] Copyright 2019, American Chemical Society. c) Electrochemical redox mechanism of polyimide and the cell configuration. Reproduced with permission.^[61a] Copyright 2013, Elsevier B.V. d) Schematic illustration of the simplified structure of a fiber-shaped aqueous lithium battery using polyimide (PI)/carbon nanotube as the anode. e) SEM image of PI/CNT fiber. f) Rate capability of the PI/CNT fiber anode. Reproduced with permission.^[62c] Copyright 2016, The Royal Society of Chemistry.

boost rate performance, but their cycling instability is the biggest obstacle to their application in aqueous batteries. The vulnerability of their layered structure and the dissolution of transition-metal ions in aqueous solution are the major factors resulting in poor cycling life. The presence of their crystal water can support stacked layers and maintain their structural integrity, in which H-bonds interact between the layers.^[55] In addition, choosing stable substrate materials to synthesize composites with oxides can ensure structural stability because the substrate materials work as a buffer to accommodate the volume changes of oxides during cycling, as in the case of N-doped carbon quantum dots/ reduced graphene oxide/ iron oxide (N-CQDs/rGO/Fe₂O₃) (shown in Figure 6b).^[56] Based on these findings, future research could be focused on the combination of varied substrate materials, their fabrication, and comparison of their different morphologies. Coating is another way to improve cycling stability. For example, Liu et al. proposed MoO₃ coated with polypyrrole.^[57] The polypyrrole coating could not only inhibit the dissolution of molybdenum ions, but also buffer the possible volume changes during cycling. It should be noted that the fast capacity fading of oxide anodes is partly attributable to the irreversible phase transition that mainly occurs in the first discharge.^[55c] There has been little research, however, that could offer a comprehensive understanding of

the relationship between the complicated phase transitions and elemental composition in aqueous batteries.

Compared with conventional inorganic anode materials, organic anodes, such as conductive polymers and carbonyl compounds, possess satisfactory working voltages, high and robust stability, structural diversity, design flexibility, and abundant raw materials that are low-cost and environmentally benign, corresponding to excellent electrochemical properties. The exploration of conductive polymers such as polyaniline (PANI) and polypyrrole (PPy) is in its infancy because their limited doping level restricts high capacity.^[58] In contrast, carbonyls and their derivatives can deliver a much higher charge capacity, but their rate and cycling performances are greatly plagued by their intrinsic poor electronic conductivity and high solubility in aqueous electrolytes. For example, there are no reports related to carboxylate group-based organic anodes for aqueous batteries due to their inherent soluble nature in aqueous solution, although considerable research efforts have been devoted to exploring these anodes in nonaqueous batteries, such as di-lithium terephthalate and di-lithium trans-trans-muconate for lithium batteries, and disodium terephthalate and sodium terephthalate for sodium batteries as low-cost and high-performance anode materials.^[59] The application of carbonyl radicals, such as tetrahydroxybenzoquinone

(THBQ) and (2,2,6,6-tetramethylpiperidin-1-yl)oxyl (TEMPO) radicals has been significantly limited due to their poor electron transport capability and high solubility in aqueous electrolytes, even though they contain one or more redox-active radicals and undergo multi-electron reversible electrochemical reactions, leading to high energy density.^[60] Hydrophilic group moieties such as ammonium cations can result in water-solubility for these polymers. To suppress the dissolution of small organic molecules and their discharge products, polymerization (Figure 6c) and highly concentrated or solid-state electrolytes have been applied to stabilize structures by strengthening polymer backbones or decreasing the content of free water molecules.^[20a,61] Composites of carbonyl compounds and high conductivity materials such as carbon, graphene, and their analogues, hybrid anodes incorporating a conductive framework, using Nafion film as the separator,^[4] and substitution at N-sites are effective approaches to enhance rate performance.^[62] Based on these strategies, further investigations could focus on optimizing high conductivity materials, including choosing carbon nanotubes, dispersing alloxazine (ALO) in the nanochannels of mesoporous carbon (CMK-3), and engineering 3D fibers.^[62a–62c] More specifically, nanocomposites of ALO and CMK-3 were prepared by a simple impregnation method. The introduction of CMK-3 as the matrix could improve the electrical conductivity of ALO and further reduce the dissolution of sodiated ALO due to its high conductivity, well-ordered porous network, and large pore volume.^[62b] Polyimide (PI)/carbon nanotube (CNT) hybrid fibers have also been designed as the anode for aqueous lithium-ion batteries. CNT fibers with a uniform diameter along their length direction were spun from a CNT array synthesized by chemical vapor deposition, the as-spun fibers are highly aligned along the spiral direction, resulting in high electrical conductivity and tensile strength. PI was then coated on the surface of the aligned CNT fibers by in-situ polymerization for 6–8 h to form a skin–core structure, as shown in Figure 6d,e. This unique fiber structure endowed the anode with high rate capacity under ultrafast charge and discharge rates (Figure 6f).^[62c] It is well known that long-range ordered skeletons and nanopores could facilitate ion and electron transport, so more future research should be focused on developing ideal structures and morphologies and establishing the structure/morphology–electrochemical performance relationship through experimental data and first-principles calculations.

4. The Narrow Electrochemical Stability Window of Aqueous Electrolytes

The application of aqueous batteries (ABs) is always impeded by their narrow electrochemical stability window (ESW) of 1.23 V, leading to limited choices of anode and cathode materials. The recent discoveries of “water-in-salt” electrolytes (WiSE) and “water-in-bisalt” (WiBS) electrolytes have led to proposals to expand the voltage window by reducing the amount of free water molecules that can solvate cations (as illustrated in Figure 7a) and form a solid-electrolyte interphase (SEI) by anion reduction on the anode surface.^[63] High-concentration electrolytes strongly depend on the solubility of the chosen salts, however, so to increase the salt

proportion in aqueous solution, mixed-anion and mixed-cation (Na–K and Na–Li) salt electrolytes have been explored.^[64] Hydrate melt $\text{Li}(\text{TFSI})_{0.7}(\text{BETI})_{0.3} \cdot 2\text{H}_2\text{O}$ electrolyte, where TFSI^- is bis(trifluoromethane)sulfonimide and BETI^- is bis(pentafluoroethanesulfonyl)imide, achieved a wider ESW of 3.8 V,^[65] and then monohydrate melt $\text{Li}(\text{PTFSI})_{0.6}(\text{TFSI})_{0.4} \cdot \text{H}_2\text{O}$ electrolyte, where PTFSI^- is (pentafluoroethanesulfonyl)(trifluoromethane-sulfonyl)imide, further expanded the ESW to nearly 5 V because of the higher solubility and the ionic liquids of asymmetric PTFSI^- imide anions in comparison with symmetric imide anions (TFSI^- and BETI^-).^[66] Although the mixed alkali cation solutions can achieve higher salt concentrations compared to the mixed anion solutions, the presence of other alkali cations is likely to induce undesirable cation intercalation. Therefore, inert cations such as tetraethylammonium (TEA^+) and asymmetric ammonium (42 m $\text{LiTFSI} + 21$ m $\text{Me}_3\text{EtN} \cdot \text{TFSI}$),^[67] where Me_3EtN is ethyl trimethylammonium, were introduced into WiSE systems to minimize the negative effects associated with the possible intercalation of other alkali cations, since large inert cations demonstrate inertness toward intercalation in electrodes. In addition, incorporation of WiBS in a polymer matrix has led to the development of “water-in-salt” gel polymer electrolytes, for example, a concentrated-WiBS-based aqueous gel polymer electrolyte (C-W-GPE), which could expand the stable electrochemical window to 4.1 V by decreasing the water activity through coordinating with hydroxyl-group-rich polymers and increasing the Li salt content due to its high solubility in the monomer.^[68]

The concept of WiSE and hydrate-melt electrolytes has been extensively applied in aqueous potassium and sodium batteries.^[63c,69] A relatively wide ESW of 2.5 V was achieved in 9.26 m NaCF_3SO_3 WiSE, where a Na^+ -conducting SEI was formed on the anode surface to effectively suppress hydrogen evolution. Molecular modelling reveals a more pronounced ion aggregation with frequent contact between the sodium cation and the fluorine-containing anion as one of the main factors responsible for the formation of a dense SEI at a lower salt concentration than its Li counterpart.^[63a] Furthermore, the newly discovered $\text{Na}(\text{PTFSI})_{0.65}(\text{TFSI})_{0.14}(\text{OTf})_{0.21} \cdot 3\text{H}_2\text{O}$ and $\text{K}(\text{PTFSI})_{0.12}(\text{TFSI})_{0.08}(\text{OTf})_{0.8} \cdot 2\text{H}_2\text{O}$ hydrate melts can significantly extend the potential window up to 2.7 and 2.5 V, respectively, owing to their advantage that almost all water molecules participate in the Na^+ or K^+ hydration shells.^[69b] Although the ESW is slightly narrower in aqueous sodium and potassium batteries than that in lithium ion batteries, the high ionic conductivity of aqueous sodium and potassium electrolytes, their high abundance on earth, and their low cost make them more attractive for large-scale energy storage. The use of high-concentrated fluorinated salts, however, might counteract the advantages of aqueous batteries due to their high cost and toxicity. To address these issues, low-cost and environmentally friendly WiSEs based on mixed cation acetates (32 m $\text{KAc} + 8$ m NaAc) and low-cost inorganic salts have been developed.^[70] Unlike the formation of SEI layers in organic salt electrolytes, the expanded ESW with inorganic salts is mainly attributed to the kinetic contribution, which originates from their unique local structures. Through comprehensively studying the solution structure of LiNO_3 , self-assembly behavior in electrolytes has been identified, proceeding from isolated Li^+

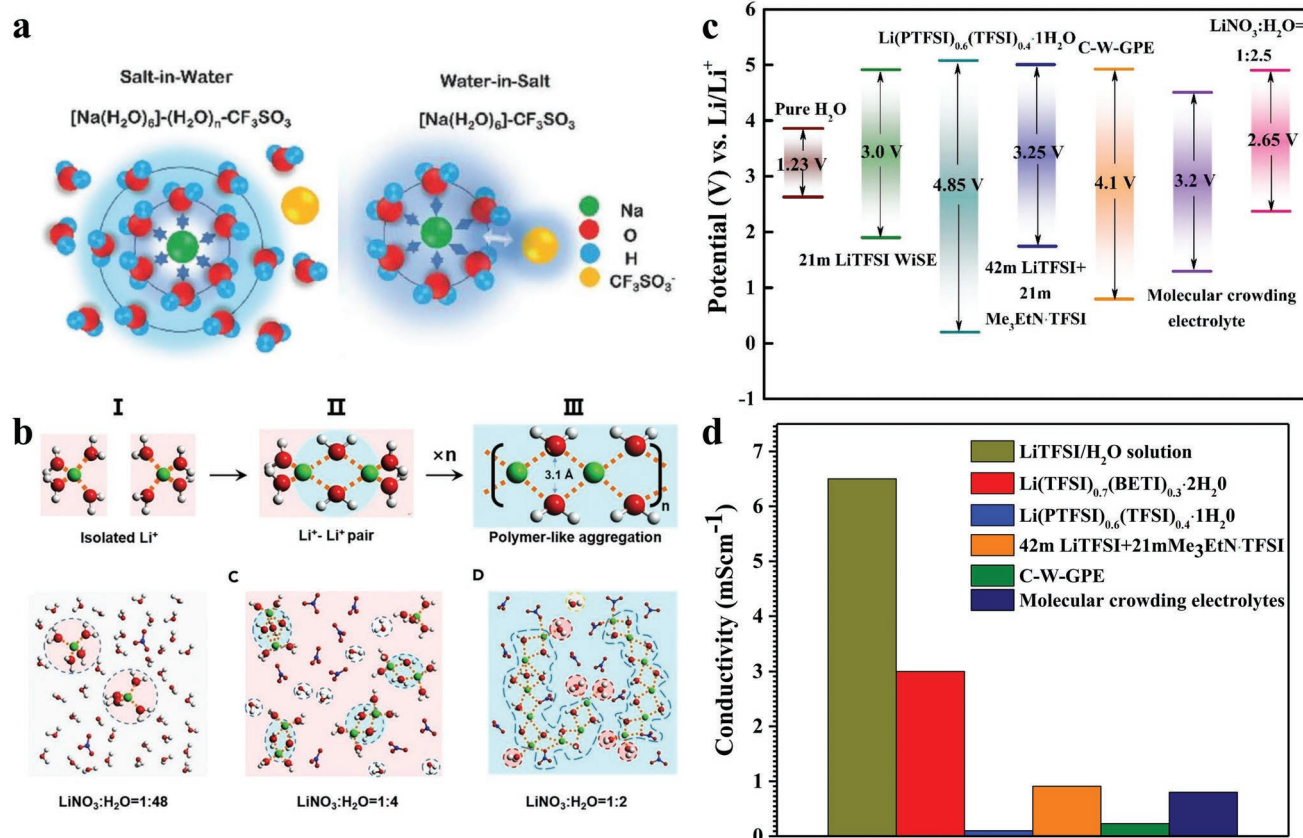


Figure 7. a) Illustration of the evolution of the Na^+ primary solvation sheath in diluted and water-in-salt solutions. Reproduced with permission.^[63] Copyright 2017, WILEY-VCH. b) Schematic snapshots of 2 m LiTFSI-94%PEG-6% H_2O and 2 m LiTFSI- H_2O electrolyte during molecular dynamics (MD) simulations. Reproduced with permission.^[71] Copyright 2018, Elsevier Inc. Comparison of electrochemical properties in aqueous lithium batteries using different strategies: c) electrochemical stability windows and d) ionic conductivity.

with a first solvation sheath to linear aggregation between Li^+ and then $(\text{Li}^+(\text{H}_2\text{O})_2)_n$ polymer-like chains (Figure 7b) as the salt concentration increases. In such polymer-like aggregations, the resistance of water molecules to oxidation is significantly improved, as their OH groups are occupied by intimate $\text{Li}^+\text{-OH}$ (water-oxygen) interactions.^[71] Moreover, the potential window of a series of inorganic Li and Na salt-containing concentrated electrolytes with neutral pH was investigated from the viewpoint of the local pH change and water concentration, highlighting the importance of local pH change, which can expand the potential windows in unbuffered neutral pH solutions.^[72] On the other hand, improvement of the voltage window with low salt concentrations has been a popular strategy. A “molecular crowding” electrolyte using the water-miscible polymer poly(ethylene glycol) (PEG) as the crowding agent was proposed to substantially reduce the concentration of free water molecules through altering the hydrogen-bonding structure, thereby achieving a 3.2 V ESW with a low salt concentration (2 m).^[73] As shown in Figures 7c and 7d, we compared the ESW and ionic conductivity of aqueous lithium batteries using different strategies, which could lead to the employment of more anode and cathode materials to be used in aqueous battery systems.

Introducing an electrolyte additive has been considered as another practical approach to improving the electrochemical

properties.^[74] Tris(trimethylsilyl) borate (TMSB) added to WiSE could decompose and form a cathode electrolyte interphase (CEI) on a LiCoO_2 surface, since TMSB possesses the highest HOMO level, so it can be the first to be oxidized before water or salt anions (as shown in Figure 8a,b).^[75] The addition of dodecyl sulfate (SDS) surfactant expanded the stable voltage window to 2.5 V and stabilized the electrode structure by different mechanisms.^[76] SDS was adsorbed on the electrode surface with its hydrophilic group facing the electrode and its hydrophobic group facing the medium, which resulted in a higher energy barrier against the passage of water molecules through the dense hydrophobic layer than carrier ions (Figure 8c,d). This effectively suppressed the evolution of oxygen and maintained the pH of the electrolyte, inhibiting the dissolution of transition metal from the electrode materials in acidic electrolyte due to the decomposition of water. Because the OER and HER are surface reactions and the reduction or oxidation stability is significantly affected by the surface properties of the electrode, an artificial layer on the electrode surface is an effective strategy to reduce the contact between the electrode and aqueous electrolytes.^[77] For instance, on the anode side, coating materials either strongly negative or highly positive with respect to the free energy of hydrogen, such as Al_2O_3 , are ideal to suppress the HER.^[78]

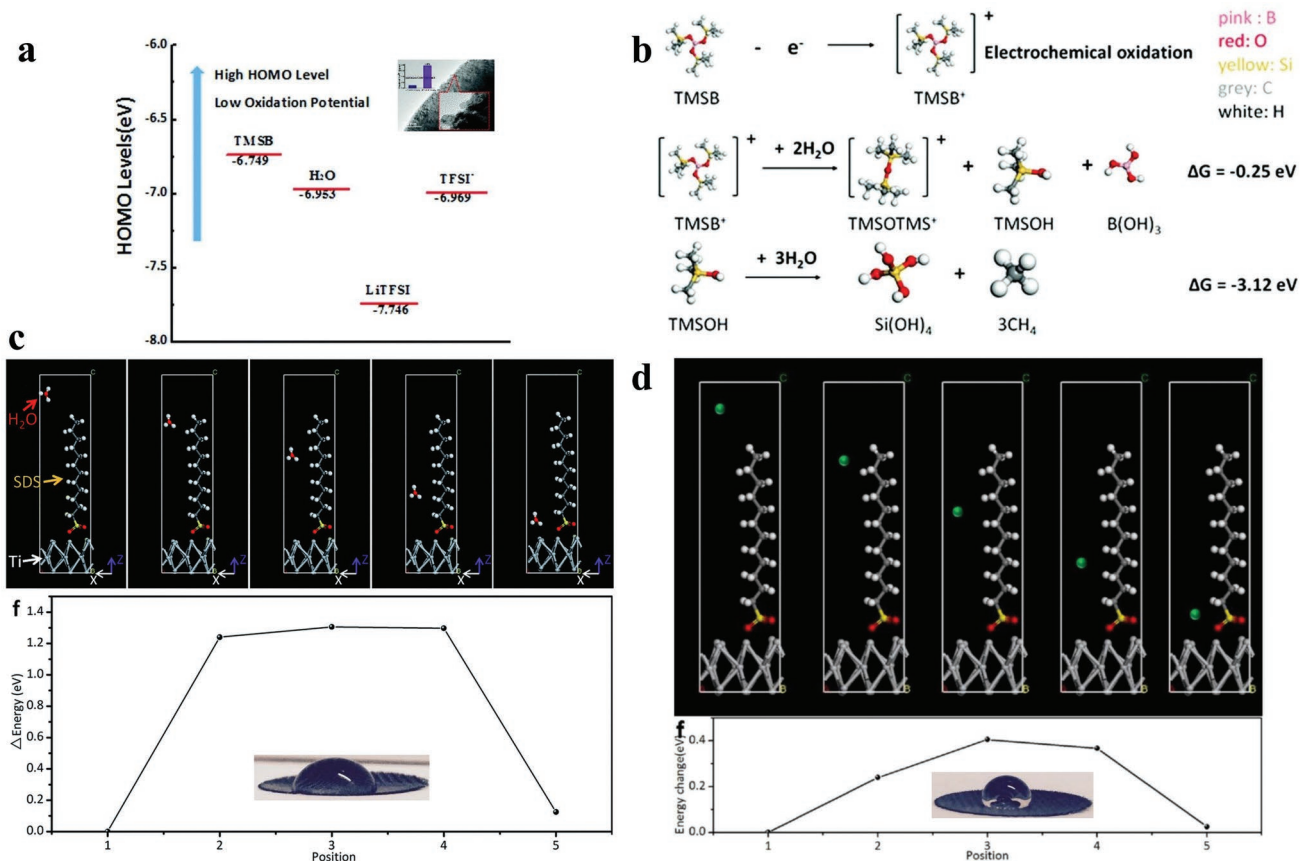


Figure 8. a) Highest occupied molecular orbital (HOMO) levels of TMSB, H₂O, LiTFSI, and TFSI⁻. b) Schematic illustration of the possible mechanisms for electrochemical oxidative decomposition of TMSB. Reproduced with permission.^[75] Copyright 2016, The Royal Society of Chemistry. Model of density functional theory calculations, showing ion passing through the SDS adsorption interlayer at different positions and the tendency of energy change of water molecules at different positions for c) water molecule and d) sodium ions. Reproduced with permission.^[76] Copyright 2017, The Royal Society of Chemistry.

5. Conclusion and Future Perspectives

In summary, this review has mainly compared the advantages and drawbacks of cathode materials (PBAs, polyanion-type compounds, and oxides), and introduced several kinds of representative anode materials and electrolytes for aqueous monovalent-ion batteries. Specifically, sodium and potassium batteries have been attracting increasing attention due to their high abundance, easy access on earth, and the high solubility of sodium and potassium salts in water, making them more desirable for the development of low-cost aqueous batteries in industrial processes, although lithium batteries possess relatively high energy density and long lifespans.^[79] Moreover, hydrated potassium ions as charge carriers in aqueous solution exhibit the fastest diffusion kinetics both in aqueous electrolytes and at electrode/electrolyte interfaces compared with hydrated lithium and sodium ions, since hydrated potassium ions possess the smallest hydrated ionic radius and hydration free energy among them, indicating the potential for fast charging capability and excellent power density (Figure 1a). Therefore, aqueous potassium batteries could be considered as a promising candidate for high power devices in large-scale energy storage systems. Herein, we aim to summarize the various

strategies to enhance their electrochemical performance for future research in terms of structural engineering, morphology control, elemental compositions, and interfacial design.

5.1. Cathode Materials

The application of cathode materials in aqueous monovalent-ion batteries has mainly been hindered by capacity fading. To overcome this challenge, the future directions that could be followed are:

- Elucidation of cathode phase transition behavior. Cathode materials generally experience complicated phase transitions in aqueous-based electrolytes, but the detailed phase transition behavior and mechanisms have been unclear, so they should be further comprehensively studied, with a particular focus on optimizing the chemical composition, especially the content of monovalent-ions, to balance the energy density and structural stability of cathode materials.
- Tailoring of the role of water molecules in the cathode lattice. Water molecules in the cathode lattice could serve as pillars to maintain the crystal structure and facilitate low

- strain during cycling. To tailor the positions and content of water molecules, novel synthesis methods such as room-temperature soaking could be employed. It is also critical to deeply understand the reaction mechanisms, which could be revealed via advanced characterization tools, thus helping to optimize experimental parameters such as the coprecipitation temperature, as well as the solvents and etching solutions.
- iii. Stabilization of the crystal structure. In terms of the crystal structure, current research has focused on cationic substitution, such as Ni or Fe to stabilize the crystal structure. Future research might be extended to other elements, such as Ti, Tb, and V, which could enhance the strength of monovalent-ion–O bonds and block the intercalation pathways for water-related species, leading to higher water-stability.
 - iv. Interfacial engineering via surface coating. Interfacial engineering has been confirmed to successfully prevent transition metal ions from dissolving into aqueous electrolytes. Optimizing the amount of surface coating materials, such as nickel hexacyanoferrate (NiHCF), poly(3,4-ethylenedioxythiophene) (PEDOT), and $\text{Na}_3(\text{VOPO}_4)_2\text{F}$,^[80] as well as multi-layer coatings with various materials to form a composite coating structure on the cathode surface, and achieving uniformity and controllability of the surface coating by novel coating technologies,^[81] such as radio frequency magnetron sputtering and spin-coating, could be worth more attention.
- ii. Suppression of the high solubility of carbonyl compounds in aqueous electrolytes. Two different strategies could be employed to achieve this goal. One is to tune the functional groups to form covalent–organic frameworks (COFs) or metal-organic frameworks (MOFs). COFs allow precise integration of the redox-active building blocks into 2D or 3D polymeric frameworks with long-range ordered skeletons and nanopores via in-situ polymerization or a facile and scalable mechanical milling method.^[83] In the case of MOFs, the active organic species are immobilized by metal-ligand coordinate covalent bonds. Moreover, their porous structures and electrical conductivity can improve the rate capability, which is beneficial for achieving high-power energy storage. The choice of metal chelation is quite vital in the synthesis process, and 2,3,6,7,10,11-hexahydroxytriphenylene has been employed to increase the chemical stability in aqueous solution, as well as the thermal stability and porosity of MOFs.^[84] The other option is the introduction of hydrophobic groups into the molecular backbone. This type of hyperbranched polymer could be synthesized through proton transfer polymerization of diglycidyl ethers, cationic polymerization, or anionic polymerization of propylene oxide and glycidol.^[85]
 - iii. Understanding the electrochemical reaction mechanisms of organic materials during cycling. These have not been well studied to date, so it is essential to achieve a comprehensive understanding to help researchers to establish the structure/morphology–electrochemical performance relationship via the combination of experiments and theoretical calculations.

5.2. Anode Materials

Searching for potential anode materials that possess good structural stability and rate capability in aqueous electrolytes is essential for the development of aqueous monovalent-ion batteries. Polyanionic compounds, oxides, and organic materials have been well studied to date. Compared to the polyanionic compounds with inherently low electronic conductivity and oxides with vulnerable layer structures, the structural diversity and design flexibility of organic electrode materials offer more possibilities to achieve better electrochemical properties, although the research on organic anodes in aqueous batteries is currently at a very early stage. Many critical issues still need to be solved in the search for new anodes. These include:

- i. The exploration of organic anodes for application in aqueous electrolytes. This has mainly focused on conductive polymers and carbonyl compounds, but the limited doping levels of conductive polymers and the intrinsically poor electronic conductivity as well as the high solubility of carbonyl compounds in aqueous electrolytes have greatly hindered their application. Therefore, it is necessary to investigate the huge potential of other organic materials, such as organic radicals with stable structures and electron delocalization.^[82] Future research should be focused on improving their theoretical specific capacity due to their heavy repeating units, such as by synthesizing organic radicals with more compact functional groups.

5.3. Electrochemical Stability Window

The narrow ESW of aqueous electrolytes greatly limits the choice of electrode materials, leading to poor energy density. Numerous attempts in the past several years have been focused on expanding the ESW by suppressing the HER and OER. Future optimization of these strategies could involve:

- i. In the case of organic salts, highly-concentrated electrolytes have been extensively applied. Considering the high cost and toxicity of fluorinated salts, it is necessary to achieve the application of inorganic salts in aqueous electrolytes and clarify the interaction mechanisms of water molecules and cations of inorganic salts, which is a key to tailoring the local structure and optimizing their electrochemical properties.
- ii. The presence of additives in aqueous electrolytes could widen the ESW in different ways, such as by forming a protective electrolyte interphase on the cathode surface or adsorbing the additive on the electrode surface to block water molecules from coming into contact with the electrode. There are more types of additives, such as polyethylene glycol and other surfactants, which can inhibit the decomposition of water and the dissolution of transition metals, such as sodium carboxymethylcellulose, sodium dodecyl benzene sulfonate, and dodecyltrimethylammonium bromide, which might be extended to use in aqueous-based electrolytes.

- iii. Coating an artificial SEI layer on the electrode surface has been demonstrated to be an effective strategy to suppress the side reactions that take place at the electrode/electrolyte interface and also to widen the potentials of oxygen evolution and hydrogen evolution. Therefore, TiO₂ and ZnO coating materials with stable electrochemical properties could be further studied.
- iv. Although many researchers have reported that the reduction of salt anions could form a passivating SEI on the anode surface to stabilize the voltage window in highly-concentrated aqueous electrolytes, the chemistry and formation mechanisms of such aqueous SEI layers and the mechanism of ion transport through the SEI have remained virtually unknown. Future attempts could be focused on controlling the irreversible reduction reaction and inhibiting the decomposition of water molecules to form a dense and protective SEI layer, as well as suppressing the dissolution and corrosion of the SEI during long-term cycling and reducing irreversible H₂-evolution.

In short, although previous strategies have been employed to greatly enhance the electrochemical performance of these components for aqueous monovalent-ion batteries, there is still a long way to go in terms of high energy cathodes, matching anodes, and stable electrolytes before it is possible to achieve future practical applications. It is hoped that this review paper could promote the transfer of the knowledge acquired in previous studies and generate some novel ideas for the future development of aqueous monovalent-ion batteries for electrochemical energy storage.

Acknowledgements

Financial support from the Australian Research Council (ARC) (LP160101629, DP210101486, and DP200101862) and the National Natural Science Foundation of China (Grant No. 52104315) is acknowledged.

Open access publishing facilitated by The University of Adelaide, as part of the Wiley - The University of Adelaide agreement via the Council of Australian University Librarians.

Conflict of Interest

The authors declare no conflict of interest.

Keywords

anodes, aqueous monovalent-ion batteries, cathodes, electrolytes, the correlations between the strategies and the performance

Received: October 5, 2021

Revised: February 25, 2022

Published online:

- [1] N. Kittner, F. Lill, D. M. Kammen, *Nat. Energy* **2017**, *2*, 17125.
 [2] a) M. Armand, J. M. Tarascon, *Nature* **2008**, *451*, 652; b) S. Zhang, W. Deng, X. Zhou, B. He, J. Liang, F. Zhao, Q. Guo, Z. Liu, *Mater. Today Energy* **2021**, *21*, 100770.

- [3] X. Dong, L. Chen, J. Liu, S. Haller, Y. Wang, Y. Xia, *Sci. Adv.* **2016**, *2*, e1501038.
 [4] L. Smith, B. Dunn, *Science* **2015**, *350*, 918.
 [5] W. Li, J. R. Dahn, D. S. Wainwright, *Science* **1994**, *264*, 1115.
 [6] a) H. Chen, E. Ruckenstein, *J. Phys. Chem. B* **2015**, *119*, 12671; b) B. Tansel, *Sep. Purif. Technol.* **2012**, *86*, 119.
 [7] a) W. Zhang, Z. Guo, *Nat. Sci. Rev.* **2021**, *8*, 043; b) B. Cao, Q. Zhang, H. Liu, B. Xu, S. Zhang, T. Zhou, J. Mao, W. K. Pang, Z. Guo, A. Li, J. Zhou, *Adv. Energy Mater.* **2018**, *8*, 1801149; c) S. Liu, J. Mao, L. Zhang, W. K. Pang, A. Du, Z. Guo, *Adv. Mater.* **2021**, *33*, 2006313; d) Y. Wang, Z. Wang, L. Zhao, Q. Fan, X. Zeng, S. Liu, W. K. Pang, Y. B. He, Z. Guo, *Adv. Mater.* **2021**, *33*, 2008133.
 [8] a) N. Alias, A. A. Mohamad, *J. Power Sources* **2015**, *274*, 237; b) Y. Shen, B. Liu, X. Liu, J. Liu, J. Ding, C. Zhong, W. Hu, *Energy Storage Mater.* **2020**, *34*, 461; c) J. Huang, Z. Guo, Y. Ma, D. Bin, Y. Wang, Y. Xia, *Small Methods* **2019**, *3*, 1800272; d) X. Zeng, J. Hao, Z. Wang, J. Mao, Z. Guo, *Energy Storage Mater.* **2019**, *20*, 410; e) J. Hao, X. Li, X. Zeng, D. Li, J. Mao, Z. Guo, *Energy Environ. Sci.* **2020**, *13*, 3917.
 [9] Y. Lu, L. Wang, J. Cheng, J. B. Goodenough, *Chem. Commun.* **2012**, *48*, 6544.
 [10] W. J. Xu, Z. Y. Du, W. X. Zhang, X. M. Chen, *CrystEngComm* **2016**, *18*, 7915.
 [11] a) J. Nai, X. W. Lou, *Adv. Mater.* **2019**, *31*, 1706825; b) R. Y. Wang, C. D. Wessells, R. A. Huggins, Y. Cui, *Nano Lett.* **2013**, *13*, 5748; c) H. W. Lee, R. Y. Wang, M. Pasta, S. W. Lee, N. Liu, Y. Cui, *Nat. Commun.* **2014**, *5*, 1.
 [12] a) D. Su, A. McDonagh, S. Z. Qiao, G. Wang, *Adv. Mater.* **2017**, *29*, 1604007; b) Q. Yang, W. Wang, H. Li, J. Zhang, F. Kang, B. Li, *Electrochim. Acta* **2018**, *270*, 96; c) M. Xia, X. Zhang, T. Liu, H. Yu, S. Chen, N. Peng, R. Zheng, J. Zhang, J. Shu, *Chem. Eng. J.* **2020**, *394*, 124923; d) W. Ren, X. Chen, C. Zhao, *Adv. Energy Mater.* **2018**, *8*, 1801413.
 [13] a) W. Zhang, Y. Zhao, V. Malgras, Q. Ji, D. Jiang, R. Qi, K. Ariga, Y. Yamauchi, J. Liu, J. S. Jiang, M. Hu, *Angew. Chem., Int. Ed.* **2016**, *55*, 8228; b) M. Hu, S. Furukawa, R. Ohtani, H. Sukegawa, Y. Nemoto, J. Reboul, S. Kitagawa, Y. Yamauchi, *Angew. Chem., Int. Ed.* **2012**, *51*, 984.
 [14] S. Park, J. Kim, S. H. Yi, S. E. Chun, *ChemSusChem* **2021**, *14*, 1082.
 [15] a) X. Wu, M. Sun, S. Guo, J. Qian, Y. Liu, Y. Cao, X. Ai, H. Yang, *ChemNanoMat* **2015**, *1*, 188; b) X. Wu, Y. Luo, M. Sun, J. Qian, Y. Cao, X. Ai, H. Yang, *Nano Energy* **2015**, *13*, 117.
 [16] a) L. Jiang, L. Liu, J. Yue, Q. Zhang, A. Zhou, O. Borodin, L. Suo, H. Li, L. Chen, K. Xu, Y. S. Hu, *Adv. Mater.* **2020**, *32*, 1904427; b) X. Wu, Y. Cao, X. Ai, J. Qian, H. Yang, *Electrochem. Commun.* **2013**, *37*, 145; c) X. Y. Wu, M. Y. Sun, Y. F. Shen, J. F. Qian, Y. L. Cao, X. P. Ai, H. X. Yang, *ChemSusChem* **2014**, *7*, 407.
 [17] a) U. A. Charles, M. A. Ibrahim, M. A. M. Teridi, *J. Power Sources* **2018**, *378*, 717; b) X. Wu, W. Deng, J. Qian, Y. Cao, X. Ai, H. Yang, *J. Mater. Chem. A* **2013**, *1*, 10130; c) M. Takachi, T. Matsuda, Y. Moritomo, *Appl. Phys. Express* **2013**, *6*, 025802.
 [18] L. Jiang, Y. Lu, C. Zhao, L. Liu, J. Zhang, Q. Zhang, X. Shen, J. Zhao, X. Yu, H. Li, X. Huang, *Nat. Energy* **2019**, *4*, 495.
 [19] a) C. Li, L. Gu, J. Tong, S. Tsukimoto, J. Maier, *Adv. Funct. Mater.* **2011**, *21*, 1391; b) S. Y. Lim, J. H. Lee, S. Kim, J. Shin, W. Choi, K. Y. Chung, D. S. Jung, J. W. Choi, *ACS Energy Lett.* **2017**, *2*, 998.
 [20] X. Guo, Z. Wang, Z. Deng, X. Li, B. Wang, X. Chen, S. P. Ong, *Chem. Mater.* **2019**, *31*, 5933.
 [21] a) J. Wang, C. Mi, P. Nie, S. Dong, S. Tang, X. Zhang, *J. Electroanal. Chem.* **2018**, *818*, 10; b) W. Li, F. Zhang, X. Xiang, X. Zhang, *J. Phys. Chem. C* **2017**, *121*, 27805.
 [22] T. Shao, C. Li, C. Liu, W. Deng, W. Wang, M. Xue, R. Li, *J. Mater. Chem. A* **2019**, *7*, 1749.
 [23] a) Z. Gong, Y. Yang, *Energy Environ. Sci.* **2011**, *4*, 3223; b) Q. Ni, Y. Bai, F. Wu, C. Wu, *Adv. Sci.* **2017**, *4*, 1600275.

- [24] A. K. Padhi, K. S. Nanjundaswamy, J. B. Goodenough, *J. Electrochem. Soc.* **1997**, *144*, 1188.
- [25] a) Y. Zhang, P. Xin, Q. Yao, *J. Alloys Compd.* **2018**, *741*, 404; b) P. R. Kumar, Y. H. Jung, C. H. Lim, D. K. Kim, *J. Mater. Chem. A* **2015**, *3*, 6271; c) P. R. Kumar, Y. H. Jung, J. E. Wang, D. K. Kim, *J. Power Sources* **2016**, *324*, 421; d) S. Liu, L. Wang, J. Liu, M. Zhou, Q. Nian, Y. Feng, Z. Tao, L. Shao, *J. Mater. Chem. A* **2019**, *7*, 248; f) P. R. Kumar, A. Kheireddine, U. Nisar, R. A. Shakoor, R. Essehli, R. Amin, I. Belharouak, *J. Power Sources* **2019**, *429*, 149.
- [26] M. Chen, W. Hua, J. Xiao, D. Cortie, X. Guo, E. Wang, Q. Gu, Z. Hu, S. Indris, X. L. Wang, S. L. Chou, *Angew. Chem.* **2020**, *132*, 2470.
- [27] a) W. Zhang, J. Mao, W. K. Pang, X. Wang, Z. Guo, *Nano Energy* **2018**, *49*, 549; b) H. He, D. Huang, Y. Tang, Q. Wang, X. Ji, H. Wang, Z. Guo, *Nano Energy* **2019**, *57*, 728; c) X. Rui, W. Sun, C. Wu, Y. Yu, Q. Yan, *Adv. Mater.* **2015**, *42*, 6670.
- [28] a) H. K. Roh, H. K. Kim, M. S. Kim, D. H. Kim, K. Y. Chung, K. C. Roh, K. B. Kim, *Nano Res.* **2016**, *9*, 1844; b) Z. Guo, Y. Zhao, Y. Ding, X. Dong, L. Chen, J. Cao, C. Wang, Y. Xia, H. Peng, Y. Wang, *Chem* **2017**, *3*, 348.
- [29] a) J. Y. Luo, Y. Y. Xia, *Adv. Funct. Mater.* **2007**, *17*, 3877; b) L. Zhang, T. Huang, A. Yu, *J. Alloys Compd.* **2015**, *646*, 522; c) Q. Zhang, C. Liao, T. Zhai, H. Li, *Electrochim. Acta* **2016**, *196*, 470.
- [30] J. Dong, G. Zhang, X. Wang, S. Zhang, C. Deng, *J. Mater. Chem. A* **2017**, *5*, 18725.
- [31] a) L. Chen, J. Liu, Z. Guo, Y. Wang, C. Wang, Y. Xia, *J. Electrochem. Soc.* **2016**, *163*, A904; b) P. He, J. L. Liu, W. J. Cui, J. Y. Luo, Y. Y. Xia, *Electrochim. Acta* **2011**, *56*, 2351; c) M. Zhao, G. Huang, W. Zhang, H. Zhang, X. Song, *Energy Fuels* **2013**, *27*, 1162; d) A. Tron, Y. N. Jo, S. H. Oh, Y. D. Park, J. Mun, *ACS Appl. Mater. Interfaces* **2017**, *9*, 12391; e) Y. Liu, C. Mi, C. Yuan, X. Zhang, *J. Electroanal. Chem.* **2009**, *628*, 73.
- [32] a) M. Shao, J. Deng, F. Zhong, Y. Cao, X. Ai, J. Qian, H. Yang, *Energy Storage Mater.* **2019**, *18*, 92; b) H. Zhang, S. Jeong, B. Qin, D. V. Carvalho, D. Buchholz, S. Passerini, *ChemSusChem* **2018**, *11*, 1382.
- [33] H. Gao, T. Zhou, Y. Zheng, Y. Liu, J. Chen, H. Liu, Z. Guo, *Adv. Energy Mater.* **2016**, *6*, 1601037.
- [34] W. Duan, M. Zhao, Y. Mizuta, Y. Li, T. Xu, F. Wang, T. Moriga, X. Song, *Phys. Chem. Chem. Phys.* **2020**, *22*, 1953.
- [35] M. D. Radin, S. Hy, M. Sina, C. Fang, H. Liu, J. Vinckeviciute, M. Zhang, M. S. Whittingham, Y. S. Meng, A. Van der Ven, *Adv. Energy Mater.* **2017**, *7*, 1602888.
- [36] a) B. M. De Boisse, D. Carlier, M. Guignard, C. Delmas, *J. Electrochem. Soc.* **2013**, *160*, A569; b) J. S. Thorne, R. A. Dunlap, M. D. Obrovac, *J. Electrochem. Soc.* **2012**, *160*, A361; c) S. Guo, P. Liu, H. Yu, Y. Zhu, M. Chen, M. Ishida, H. Zhou, *Angew. Chem., Int. Ed.* **2015**, *54*, 5894.
- [37] a) S. Komaba, N. Yabuuchi, T. Nakayama, A. Ogata, T. Ishikawa, I. Nakai, *Inorg. Chem.* **2012**, *51*, 6211; b) P. F. Wang, Y. You, Y. X. Yin, Y. G. Guo, *Adv. Energy Mater.* **2018**, *8*, 1701912.
- [38] a) H. Kim, D. H. Seo, A. Urban, J. Lee, D. H. Kwon, S. H. Bo, T. Shi, J. K. Papp, B. D. McCloskey, G. Ceder, *Chem. Mater.* **2018**, *30*, 6532; b) X. Zhang, Z. Wei, K. N. Dinh, N. Chen, G. Chen, F. Du, Q. Yan, *Small* **2020**, *16*, 2002700.
- [39] Z. Hou, X. Li, J. Liang, Y. Zhu, Y. Qian, *J. Mater. Chem. A* **2015**, *3*, 1400.
- [40] a) M. H. Han, N. Sharma, E. Gonzalo, J. C. Pramudita, H. E. A. Brand, J. L. Del Amo, T. Rojo, *J. Mater. Chem. A* **2016**, *4*, 18963; b) M. H. Han, E. Gonzalo, N. Sharma, J. M. L. del Amo, M. Armand, M. Avdeev, J. J. S. Garitaonandia, T. Rojo, *Chem. Mater.* **2016**, *28*, 106.
- [41] a) J. C. Ion, H. R. Shercliff, M. F. Ashby, *Acta Metall. Mater.* **1992**, *40*, 1539; b) Z. Lei, X. Liu, Y. Wu, H. Wang, S. Jiang, S. Wang, X. Hui, Y. Wu, B. Gault, P. Kontis, D. Raabe, *Nature* **2018**, *563*, 546.
- [42] a) S. Chu, C. Zhang, H. Xu, S. Guo, P. Wang, H. Zhou, *Angew. Chem.* **2021**, *133*, 13478; b) H. Song, X. Ou, B. Han, H. Deng, W. Zhang, C. Tian, C. Cai, A. Lu, Z. Lin, L. Chai, *Angew. Chem., Int. Ed.* **2021**, *60*, 24054.
- [43] a) M. Clites, B. W. Byles, E. Pomerantseva, *J. Mater. Chem. A* **2016**, *4*, 7754; b) M. Clites, E. Pomerantseva, *Energy Storage Mater.* **2018**, *11*, 30.
- [44] D. S. Charles, M. Feyngenson, K. Page, J. Neuefeind, W. Xu, X. Teng, *Nat. Commun.* **2017**, *8*, 15520.
- [45] a) L. Xue, Q. Zhang, X. Zhu, L. Gu, J. Yue, Q. Xia, T. Xing, T. Chen, Y. Yao, H. Xia, *Nano Energy* **2019**, *56*, 463; b) W. S. Yoon, K. B. Kim, M. G. Kim, M. K. Lee, H. J. Shin, J. M. Lee, J. S. Lee, C. H. Yo, *J. Phys. Chem. B* **2002**, *106*, 2526; c) X. Gu, J. L. Liu, J. H. Yang, H. J. Xiang, X. G. Gong, Y. Y. Xia, *J. Phys. Chem. C* **2011**, *115*, 12672.
- [46] a) Y. Liu, Y. Qiao, W. Zhang, H. Xu, Z. Li, Y. Shen, L. Yuan, X. Hu, X. Dai, Y. Huang, *Nano Energy* **2014**, *5*, 97; b) Y. Liu, Y. Qiao, X. Lou, X. Zhang, W. Zhang, Y. Huang, *ACS Appl. Mater. Interfaces* **2016**, *8*, 14564.
- [47] a) J. Senčanski, D. Bajuk-Bogdanović, D. Majstorović, E. Tchernychova, J. Papan, M. Vujković, *J. Power Sources* **2017**, *342*, 690; b) T. Deng, X. Fan, J. Chen, L. Chen, C. Luo, X. Zhou, J. Yang, S. Zheng, C. Wang, *Adv. Funct. Mater.* **2018**, *28*, 1800219; c) B. S. Kumar, A. Pradeep, A. Dutta, A. Mukhopadhyay, *J. Mater. Chem. A* **2020**, *8*, 18064; d) F. Gu, T. Sun, X. Yao, M. Shui, J. Shu, *J. Phys. Chem. Solids* **2021**, *149*, 109771.
- [48] H. Gao, J. B. Goodenough, *Angew. Chem.* **2016**, *128*, 12960.
- [49] a) Z. He, Y. Jiang, J. Zhu, Y. Li, Z. Jiang, H. Zhou, W. Meng, L. Wang, L. Dai, *J. Alloys Compd.* **2018**, *731*, 32; b) W. Zhang, J. Mao, S. Li, Z. Chen, Z. Guo, *J. Am. Chem. Soc.* **2017**, *139*, 3316; c) D. Sun, Y. Jiang, H. Wang, Y. Yao, G. Xu, K. He, S. Liu, Y. Tang, Y. Liu, X. Huang, *Sci. Rep.* **2015**, *5*, 10733; d) J. Zhang, L. Chen, L. Niu, P. Jiang, G. Shao, Z. Liu, *ACS Appl. Mater. Interfaces* **2019**, *11*, 39757; e) S. Chong, L. Sun, C. Shu, S. Guo, Y. Liu, W. A. Wang, H. K. Liu, *Nano Energy* **2019**, *63*, 103868; f) F. Yang, H. Gao, J. Hao, S. Zhang, P. Li, Y. Liu, J. Chen, Z. Guo, *Adv. Funct. Mater.* **2019**, *29*, 1808291.
- [50] B. Zhao, Q. Wang, S. Zhang, C. Deng, *J. Mater. Chem. A* **2015**, *3*, 12089.
- [51] W. Zhang, W. K. Pang, V. Sencadas, Z. Guo, *Joule* **2018**, *2*, 1534.
- [52] a) Z. He, Y. Jiang, W. Meng, J. Zhu, Y. Liu, L. Dai, L. Wang, *Electrochim. Acta* **2016**, *222*, 1491; b) D. Sun, X. Xue, Y. Tang, Y. Jing, B. Huang, Y. Ren, Y. Yao, H. Wang, G. Cao, *ACS Appl. Mater. Interfaces* **2015**, *7*, 28337; c) G. M. Weng, L. Y. S. Tam, Y. C. Lu, *J. Mater. Chem. A* **2017**, *5*, 11764; d) W. Zhang, C. Hu, Z. Guo, L. Dai, *Angew. Chem., Int. Ed.* **2020**, *59*, 3470; e) Z. He, Y. Jiang, J. Zhu, H. Wang, Y. Li, H. Zhou, W. Meng, L. Dai, L. Wang, *Electrochim. Acta* **2018**, *279*, 279; f) L. Li, Y. Wen, H. Zhang, H. Ming, J. Pang, P. Zhao, G. Cao, *ChemElectroChem* **2019**, *6*, 1908; g) W. Zhang, B. W. Zhang, *Nano-Micro Lett.* **2021**, *13*, 1.
- [53] a) X. Li, X. Zhu, J. Liang, Z. Hou, Y. Wang, N. Lin, Y. Zhu, Y. Qian, *J. Electrochem. Soc.* **2014**, *161*, A1181; b) D. Sun, G. Jin, Y. Tang, R. Zhang, X. Xue, X. Huang, H. Chu, H. Wang, *J. Electrochem. Soc.* **2016**, *163*, A1388.
- [54] Z. Jiang, Y. Li, J. Zhu, B. Li, C. Li, L. Wang, W. Meng, Z. He, L. Dai, *J. Alloys Compd.* **2019**, *791*, 176.
- [55] a) H. Li, T. Zhai, P. He, Y. Wang, E. Hosono, H. Zhou, *J. Mater. Chem.* **2011**, *21*, 1780; b) D. Zhou, S. Liu, H. Wang, G. Yan, *J. Power Sources* **2013**, *227*, 111; c) C. Deng, S. Zhang, Z. Dong, Y. Shang, *Nano Energy* **2014**, *4*, 49.
- [56] X. Yun, J. Li, X. Chen, H. Chen, L. Xiao, K. Xiang, W. Chen, H. Liao, Y. Zhu, *ACS Appl. Mater. Interfaces* **2019**, *11*, 36970.
- [57] Y. Liu, B. H. Zhang, S. Y. Xiao, L. L. Liu, Z. B. Wen, Y. P. Wu, *Electrochim. Acta* **2014**, *116*, 512.
- [58] a) C. Han, R. Shi, D. Zhou, H. Li, L. Xu, T. Zhang, J. Li, F. Kang, G. Wang, B. Li, *ACS Appl. Mater. Interfaces* **2019**, *11*, 15646; b) L. Liu, F. Tian, M. Zhou, H. Guo, X. Wang, *Electrochim. Acta* **2012**, *70*, 360;

- c) M. Pasta, C. D. Wessells, R. A. Huggins, Y. Cui, *Nat. Commun.* **2012**, 3, 1149.
- [59] a) M. Armand, S. Grugeon, H. Vezin, S. Laruelle, P. Ribière, P. Poizot, J. M. Tarascon, *Nat. Mater.* **2009**, 8, 120; b) L. Zhao, J. Zhao, Y. S. Hu, H. Li, Z. Zhou, M. Armand, L. Chen, *Adv. Energy Mater.* **2012**, 2, 962; c) Y. Park, D. S. Shin, S. H. Woo, N. S. Choi, K. H. Shin, S. M. Oh, K. T. Lee, S. Y. Hong, *Adv. Mater.* **2012**, 24, 3562.
- [60] a) Y. Wang, X. Li, L. Chen, Z. Xiong, J. Feng, L. Zhao, Z. Wang, Y. Zhao, *Carbon* **2019**, 155, 445; b) T. Janoschka, N. Martin, U. Martin, C. Friebe, S. Morgenstern, H. Hiller, M. D. Hager, U. S. Schubert, *Nature* **2015**, 527, 78.
- [61] a) H. Qin, Z. P. Song, H. Zhan, Y. H. Zhou, *J. Power Sources* **2014**, 249, 367; b) L. Chen, W. Li, Z. Guo, Y. Wang, C. Wang, Y. Che, Y. Xia, *J. Electrochem. Soc.* **2015**, 162, A1972.
- [62] a) T. Gu, M. Zhou, M. Liu, K. Wang, S. Cheng, K. Jiang, *RSC Adv.* **2016**, 6, 53319; b) L. Zhong, Y. Lu, H. Li, Z. Tao, J. Chen, *ACS Sustainable Chem. Eng.* **2018**, 6, 7761; c) Y. Zhang, Y. Wang, L. Wang, C. M. Lo, Y. Zhao, Y. Jiao, G. Zheng, H. Peng, *J. Mater. Chem. A* **2016**, 4, 9002; d) D. J. Kim, Y. H. Jung, K. K. Bharathi, S. H. Je, D. K. Kim, A. Coskun, J. W. Choi, *Adv. Energy Mater.* **2014**, 4, 1400133; e) Y. Wang, X. Cui, Y. Zhang, L. Zhang, X. Gong, G. Zheng, *Adv. Mater.* **2016**, 28, 7626.
- [63] a) L. Suo, O. Borodin, T. Gao, M. Olguin, J. Ho, X. Fan, C. Luo, C. Wang, K. Xu, *Science* **2015**, 350, 938; b) L. Suo, O. Borodin, W. Sun, X. Fan, C. Yang, F. Wang, T. Gao, Z. Ma, M. Schroeder, A. von Cresce, S. M. Russell, *Angew. Chem.* **2016**, 128, 7252; c) L. Suo, O. Borodin, Y. Wang, X. Rong, W. Sun, X. Fan, S. Xu, M. A. Schroeder, A. V. Cresce, F. Wang, C. Yang, *Adv. Energy Mater.* **2017**, 7, 1701189.
- [64] X. Zeng, J. Liu, J. Mao, J. Hao, Z. Wang, S. Zhou, C. D. Ling, Z. Guo, *Adv. Energy Mater.* **2020**, 10, 1904163.
- [65] Y. Yamada, K. Usui, K. Sodeyama, S. Ko, Y. Tateyama, A. Yamada, *Nat. Energy* **2016**, 1, 16129.
- [66] S. Ko, Y. Yamada, K. Miyazaki, T. Shimada, E. Watanabe, Y. Tateyama, T. Kamiya, T. Honda, J. Akikusa, A. Yamada, *Electrochem. Commun.* **2019**, 104, 106488.
- [67] L. Chen, J. Zhang, Q. Li, J. Vatamanu, X. Ji, T. P. Pollard, C. Cui, S. Hou, J. Chen, C. Yang, L. Ma, *ACS Energy Lett.* **2020**, 5, 968.
- [68] a) C. Yang, X. Ji, X. Fan, T. Gao, L. Suo, F. Wang, W. Sun, J. Chen, L. Chen, F. Han, L. Miao, *Adv. Mater.* **2017**, 29, 1701972; b) S. A. Langevin, B. Tan, A. W. Freeman, J. C. Gagnon, C. M. Hoffman, M. W. Logan, J. P. Maranchi, K. Gerasopoulos, *Chem. Commun.* **2019**, 55, 13085.
- [69] a) R. S. Kühnel, D. Reber, C. Battaglia, *ACS Energy Lett.* **2017**, 2, 2005; b) Q. Zheng, S. Miura, K. Miyazaki, S. Ko, E. Watanabe, M. Okoshi, C. P. Chou, Y. Nishimura, H. Nakai, T. Kamiya, T. Honda, *Angew. Chem.* **2019**, 131, 14340.
- [70] J. Han, M. Zarrabeitia, A. Mariani, Z. Jusys, M. Hekmatfar, H. Zhang, D. Geiger, U. Kaiser, R. J. Behm, A. Varzi, S. Passerini, *Nano Energy* **2020**, 77, 105176.
- [71] J. Zheng, G. Tan, P. Shan, T. Liu, J. Hu, Y. Feng, L. Yang, M. Zhang, Z. Chen, Y. Lin, J. Lu, *Chem* **2018**, 4, 2872.
- [72] Y. Yokoyama, T. Fukutsuka, K. Miyazaki, T. Abe, *J. Electrochem. Soc.* **2018**, 165, A3299.
- [73] J. Xie, Z. Liang, Y. C. Lu, *Nat. Mater.* **2020**, 19, 1006.
- [74] a) X. Zeng, J. Mao, J. Hao, J. Liu, S. Liu, Z. Wang, Y. Wang, S. Zhang, T. Zheng, J. Liu, P. Rao, Z. Guo, *Adv. Mater.* **2021**, 33, 2007416; b) X. Tang, W. C. Zhang, L. Y. Cao, *Rare Met.* **2022**, 41, 726; c) W. Zhang, Y. Liu, Z. Guo, *Sci. Adv.* **2019**, 5, 7412.
- [75] F. Wang, Y. Lin, L. Suo, X. Fan, T. Gao, C. Yang, F. Han, Y. Qi, K. Xu, C. Wang, *Energy Environ. Sci.* **2016**, 9, 3666.
- [76] Z. Hou, X. Zhang, X. Li, Y. Zhu, J. Liang, Y. Qian, *J. Mater. Chem. A* **2017**, 5, 730.
- [77] a) J. Zhi, A. Z. Yazdi, G. Valappil, J. Haime, P. Chen, *Sci. Adv.* **2017**, 3, 1701010; b) F. Wang, C. F. Lin, X. Ji, G. W. Rubloff, C. Wang, *J. Mater. Chem. A* **2020**, 8, 14921.
- [78] K. Leung, Y. Qi, K. R. Zavadil, Y. S. Jung, A. C. Dillon, A. S. Cavanagh, S. H. Lee, S. M. George, *J. Am. Chem. Soc.* **2011**, 133, 14741.
- [79] W. Zhang, J. Lu, Z. Guo, *Mater. Today* **2021**, 50, 400.
- [80] a) B. Paulitsch, J. Yun, A. S. Bandarenka, *ACS Appl. Mater. Interfaces* **2017**, 9, 8107; b) X. Wang, B. Wang, Y. Tang, B. B. Xu, C. Liang, M. Yan, Y. Jiang, *J. Mater. Chem. A* **2020**, 8, 3222; c) F. Peng, L. Yu, S. Yuan, X. Z. Liao, J. Wen, G. Tan, F. Feng, Z. F. Ma, *ACS Appl. Mater. Interfaces* **2019**, 11, 37685.
- [81] a) J. Hao, B. Li, X. Li, X. Zeng, S. Zhang, F. Yang, S. Liu, D. Li, C. Wu, Z. Guo, *Adv. Mater.* **2020**, 32, 2003021; b) J. Hao, X. Li, S. Zhang, F. Yang, X. Zeng, S. Zhang, G. Bo, C. Wang, Z. Guo, *Adv. Funct. Mater.* **2020**, 30, 2001263; c) J. Long, J. Gu, Z. Yang, J. Mao, J. Hao, Z. Chen, Z. Guo, *J. Mater. Chem. A* **2019**, 7, 17854.
- [82] K. Oyaizu, T. Kawamoto, T. Suga, H. Nishide, *Macromolecules* **2010**, 43, 10382.
- [83] a) Z. Luo, L. Liu, J. Ning, K. Lei, Y. Lu, F. Li, J. Chen, *Angew. Chem., Int. Ed.* **2018**, 57, 9443; b) S. Wang, Q. Wang, P. Shao, Y. Han, X. Gao, L. Ma, S. Yuan, X. Ma, J. Zhou, X. Feng, B. Wang, *J. Am. Chem. Soc.* **2017**, 139, 4258.
- [84] a) K. W. Nam, S. S. Park, R. Dos Reis, V. P. Dravid, H. Kim, C. A. Mirkin, J. F. Stoddart, *Nat. Commun.* **2019**, 10, 4948; b) M. Hmadeh, Z. Lu, Z. Liu, F. Gándara, H. Furukawa, S. Wan, V. Augustyn, R. Chang, L. Liao, F. Zhou, E. Perre, *Chem. Mater.* **2012**, 24, 3511.
- [85] a) Z. Jia, H. Chen, X. Zhu, D. Yan, *J. Am. Chem. Soc.* **2006**, 128, 8144; b) Y. Xia, Y. Wang, Y. Wang, D. Wang, H. Deng, Y. Zhuang, D. Yan, B. Zhu, X. Zhu, *Macromol. Chem. Phys.* **2011**, 212, 1056; c) M. Schömer, J. Seiwert, H. Frey, *ACS Macro Lett.* **2012**, 1, 888.



Wenchao Zhang is currently working as a Professor at the School of Metallurgy and Environment, Central South University. He earned his Ph.D. degree in Materials Engineering under the supervision of Zaiping Guo from the University of Wollongong in 2019. He was a Visiting Scholar under the supervision of Liming Dai in the Department of Macromolecular Science and Engineering, Case Western Reserve University, USA. His current research interests are focused on fundamental understanding of heavy metal and organic pollutant treatments via electrochemical methods.



Zaiping Guo is currently a Professor at the School of Chemical Engineering and Advanced Materials, The University of Adelaide. She obtained her Ph.D. from the University of Wollongong in 2003. She was a Distinguished Professor in the school of Mechanical, Materials, Mechatronic, and Biomedical Engineering, University of Wollongong before joining the University of Adelaide. Her research is focused on the design and application of electrode materials and electrolytes for energy storage and conversion.